Molecular Design and Synthesis of Dicarbazolophane-Based Centrosymmetric through-Space Donors for Solution-Processed TADF OLEDs

Zhen Zhang,‡ Stefan Diesing,‡ Ettore Crovini, Abhishek Kumar Gupta, Eduard Spuling, Xuemin Gan, Olaf Fuhr, Martin Nieger, Zahid Hassan, Ifor D. W. Samuel,* Stefan Bräse,* and Eli Zysman-Colman*

ABSTRACT: Conjugation-extended carbazolophane donors, dicarbazolophanes (**DCCP**), were designed and synthesized by a multi-fold stepwise Pd-catalyzed Buchwald-Hartwig amination/ring cyclization process. Further, elaboration of the **DCCP** core is possible with introduction of pendant carbazole derivative groups. This provided a way of tuning the optoelectronic properties of the thermally activated delayed fluorescence (TADF) compounds **DCCPTRZtBu$_2$**, **dtBuCzDCCPTRZtBu$_2$**, and **dMeOCzDCCPTRZtBu$_2$**. Solution-processed OLEDs were fabricated and achieved maximum external quantum efficiencies (EQE_{max}) of 8.2% and EQE of 7.9% at 100 cd/m^2.

The [2.2]paracyclophane (PCP) scaffolds have been used as platforms to study both planar chirality and through-space charge mobility and electronic communication in π-stacked molecular systems.[1] The configurationally rigid structure PCP group is also photochemically stable, and chemically stable towards oxidation, acids and bases, thus making it a desirable molecular building block in organic electronics.[2] We first reported the electron-donor carbazolophane (Czp), that merges the structure of the PCP with carbazole.[3] Compared to carbazole (Cz), this donor adopts a more twisted conformation in donor-acceptor systems due to its larger size while the enlarged conjugation in the CzP results in a stronger electron donor. Further, the inherent planar chirality of the donor translates to emitters that show circularly polarized luminescence (CPL) (**Figure 1**). Incorporation of this donor produced the thermally activated delayed fluorescence (TADF) emitter **CzpPhTRZ**, which showed a small singlet-triplet energy splitting, ΔE_{ST}, of 0.16 eV and a photoluminescence quantum yield, Φ_{PL}, of 70% in 10 wt% DPEPO doped film. The organic light-emitting diodes (OLEDs) showed a maximum external quantum efficiency (EQE_{max}) of 17.0%. Zheng *et al.* reported an analog of **CzpPhTRZ** that replaced the Czp donor with a phenoxazinephane (PXZp).[4] The generated molecule, **PXZp-Ph-TRZ**, possesses a red-shifted emission and a smaller ΔE_{ST} of 0.03 eV leading to yellow TADF OLEDs with EQE_{max} of 7.8%. Very recently, we designed and synthesized two deep blue TADF emitters, **CNCzpPhTRZ** and **CF$_3$CzpPhTRZ**, through introduction of electron-withdrawing cyano (CN) and trifluoromethyl (CF_3) groups onto the Czp moiety. **CNCzpPhTRZ** and **CF$_3$CzpPhTRZ** emit at 458 and 456 nm with Φ_{PL} of 65% and 70% in 10 wt% PPT doped film, respectively.[5] Blue OLEDs exhibited EQE_{max} of 7.4% at 456 nm for **CNCzpPhTRZ,** and EQE_{max} of 11.6% at 460 nm for **CF$_3$CzpPhTRZ**. As shown in **Figure 1**, only a single deck of the PCP has been elaborated in each of these TADF emitters.

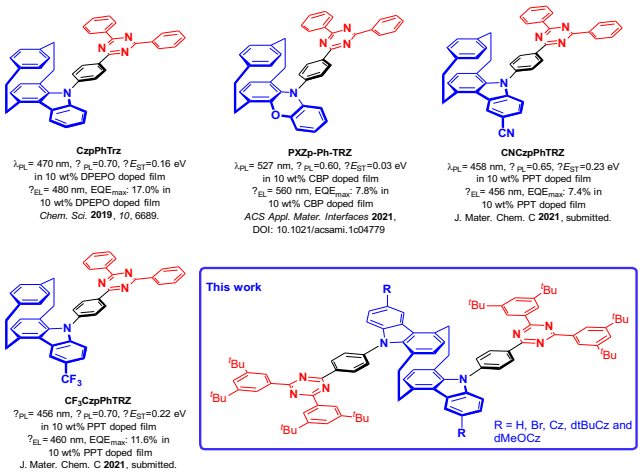

Figure 1. Chemical structures and performances of PCP-based emitters.

Here, we report the development of a new centrosymmetric through-space dicarbazolophane (**DCCP)** core, obtained through elaboration of both decks of the PCP. For the key building block, **DCCP**, we optimized a multi-gram scale efficient synthesis through a two-step protocol employing two-fold Pd-catalysed Buchwald-Hartwig amination afforded the C–N coupling product **1** with a yield of 76% (**Scheme 1**). For the synthesis of the ring cyclization product, using $Pd_2(dba)_3$ in combination with X-Phos as a catalyst system proved to be more effective for the two-fold Pd-catalysed oxidative cyclization employing the chlorinated moieties as synthetic handle.[6] **DCCP** (**2**) was obtained in a yield of 49% (2.1 g scale). **DCCP** was regio- and chemoselectively dibrominated using NBS in THF to afford **DCCP-2Br** (**3**) in 68% yield. Nucleophilic aromatic substitution with 2,4-bis(3,5-di-tert-butylphenyl)-6-(4-fluorophenyl)-1,3,5-triazine produced **DCCPTRZtBu$_2$** and the bromo-functionalized intermediate product **4** was further elaborated by grafting on

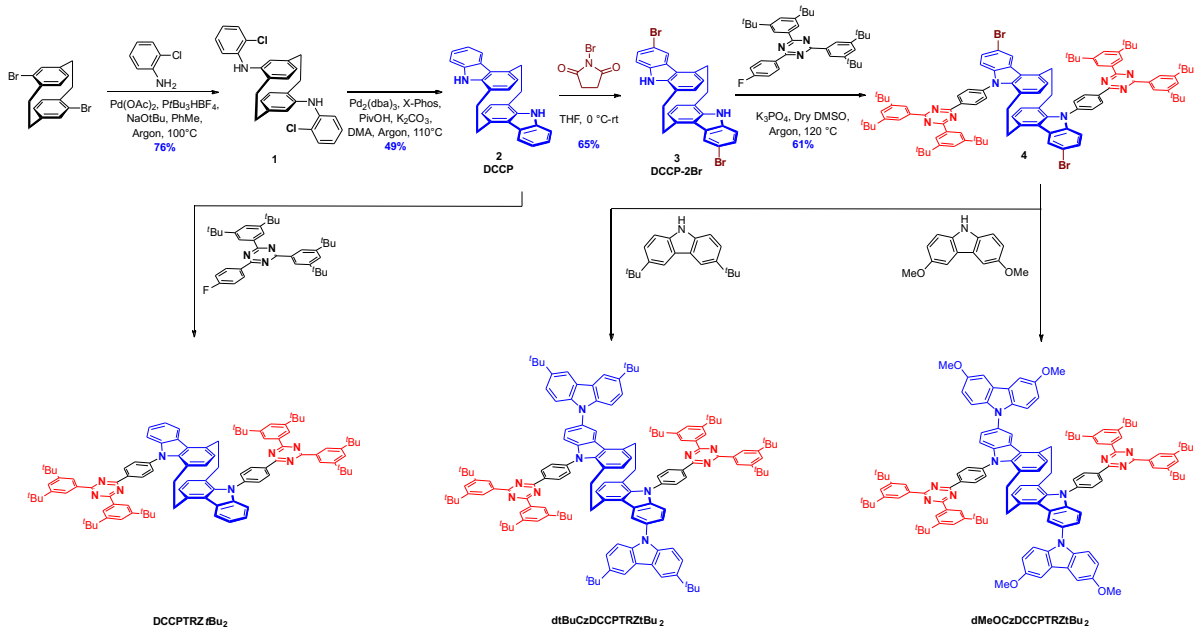

Scheme 1. Synthetic design towards dicarbazolophane-based emitters (details see ESI).

peripheral donors 3,6-di-*tert*-butyl-9*H*-carbazole (dtBuCz) and 3,6-dimethoxy-9*H*-carbazole (dMeOCz) *via* a two-fold Pd-catalyzed Buchwald-Hartwig cross-coupling to afford **dtBuCzDCCPTRZtBu$_2$** and **dMeOCzDCCPTRZtBu$_2$,** respectively. These emitters were fully characterized by NMR spectroscopy, mass spectrometry, IR spectroscopy, and Elemental analysis (EA, details see ESI).

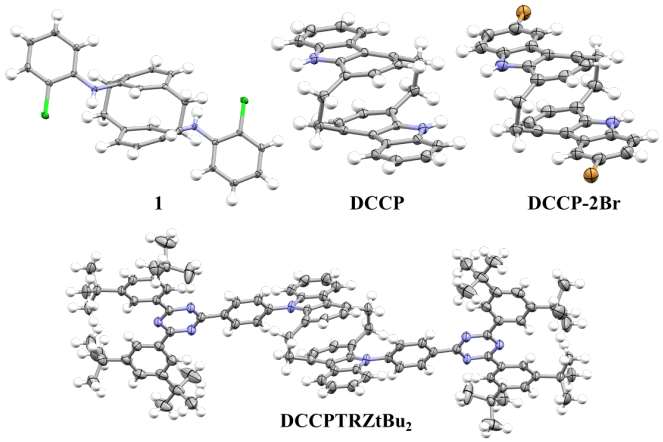

Figure 2. Thermal ellipsoid plots of the crystal structure of **1**, **DCCP**, **DCCP-2Br**, and **DCCPTRZtBu$_2$**. Ellipsoids are plotted at the 50% probability level.

The molecular structure of the compounds **1**, **DCCP**, **DCCP-2Br,** and **DCCPTRZtBu$_2$** were confirmed by single crystal X-ray analysis (**Figure 2**). The distances between the two benzene decks of the PCP are 3.01 Å for **1**, 3.03 Å for **DCCP**, 3.02 Å for **DCCP-2Br**, and 3.07 Å for **DCCPTRZtBu$_2$**, which are somewhat reduced compared to that in the parent PCP (3.09 Å).

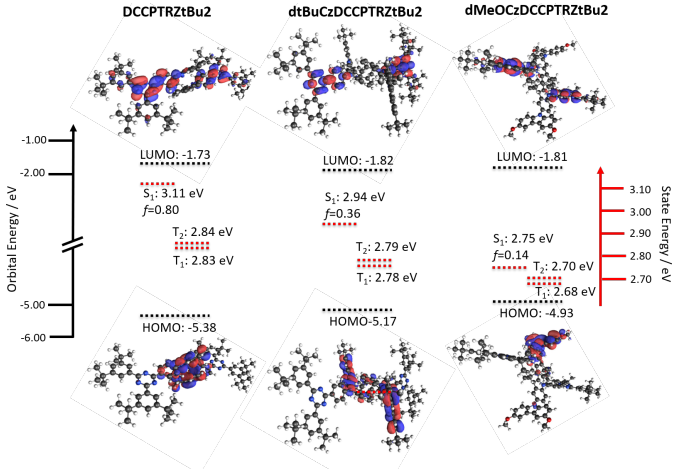

Figure 3. HOMO and LUMO electron density distribution, energy levels of excited states and oscillator strengths for the S_1-S_0 transitions of the **DCCP**-based emitters.

Theoretical calculations were employed to establish whether the **DCCP-**based emitters are likely to show TADF (**Figure 3**). The previously reported **CzpPhTrz** has a calculated HOMO level of –5.54 eV, and a ΔE_{ST} of 0.30 eV. **DCCPTRZtBu$_2$** presents a slightly smaller ΔE_{ST} of 0.28 eV and a HOMO level that is destabilized at –5.38 eV. The extended conjugation present in the **DCCP** compound results in a stronger donor character that is reflected in the shallower HOMO level. The addition of secondary substituted carbazole groups act to further increase the strength of the donor, which leads to a further destabilization of the HOMO level to –5.17 eV for **dtBuCzDCCPTRZtBu$_2$**, and –4.93 eV for **dMeOCzDCCPTRZtBu$_2$**. The singlet energy level is strongly affected by the strength of the donor, as we observe a significant decrease in its energy from 3.11 eV to 2.94 eV, to 2.75 eV with increasing strength of the donors present in

Table 1. Photophysical properties of emitters.

Compound	Toluene				PVK (10 wt%) thin film				
	λ_{PL} / nm	Φ_{PL}[a] / %	τ_p / ns	ΔE_{ST} / meV	λ_{PL} / nm	Φ_{PL}[b] / %	τ_p[c] / ns	τ_d / µs	ΔE_{ST} / meV
DCCPTRZtBu$_2$	443	91 (84)	16	330	455	41 (40)	10	--	115
dtBuCzDCCPTRZtBu$_2$	458	89 (89)	21	290	455	37 (35)	7.4	9.7	110
dMeOCzDCCPTRZtBu$_2$	475	44 (31)	29	230	490	41 (38)	6.8	7.7	70

[a] Quinine sulfate (0.5 M) in H_2SO_4 (aq) was used as the reference (Φ_{PL} = 54.6%, λ_{exc} = 360 nm). Values are given for degassed (aerated) solutions, [b] purged with nitrogen (oxygen), [c] average lifetime calculated as $\tau_{avg} = (\sum A_i \tau_i)(\sum A_i)^{-1}$.

dtBuCzDCCPTRZtBu$_2$ and **dMeOCzDCCPTRZtBu$_2$**. The triplet energy level also decreases in energy with increasing donor strength, but not as dramatically as the singlet. This leads to a decrease in ΔE_{ST} of 0.15 eV and 0.08 eV, respectively. All three materials present an intermediate triplet state that is slightly destabilized with respect to the T_1 state. As a result, the increased density of triplet states should lead to an enhancement of the RISC rates.[7]

The energy levels of the emitters were inferred from an analysis of the oxidation and reduction potentials determined by cyclic voltammetry (CV) and differential pulse voltammetry (DPV) in dichloromethane (DCM) (**Figure S22** and **Table S28**). For **DCCPTRZtBu$_2$** and **dtBuCzDCCPTRZtBu$_2$** the oxidation was found to be irreversible at a potential of 1.19 V vs. SCE and 1.09 V vs. SCE, respectively. The oxidation potential for **DCCPTRZtBu$_2$** is significantly destabilized compared to that of **CzpPhTRZ** at 1.35 V (the original value reported was 1.14 V; however, this has been revised upon re-examination of the voltammogram), thus, in line with the theoretical calculations. **dMeOCzDCCPTRZtBu$_2$** exhibits a reversible oxidation at 0.90 V vs. SCE. The substitutions at the carbazoles in the donor moiety of **dtBuCzDCCPTRZtBu$_2$** and **dMeOCzDCCPTRZtBu$_2$** lead to a destabilization of the HOMOs, resulting in the expected cathodic shift of oxidation peak potentials. This observation is confirmed by the DFT calculations. All compounds show irreversible reduction waves with a peak potential of –1.62 V, –1.78 V, and –1.72 V for **DCCPTRZtBu$_2$**, **dtBuCzDCCPTRZtBu$_2$**, and **dMeOCzDCCPTRZtBu$_2$**, respectively.

The absorption spectra (**Figure S23**), steady-state, and time-resolved photoluminescence (PL) are shown in Figure **4** and the data summarised in Table **1**. The emission spectrum in toluene is red-shifted with increasing donor strength from **DCCPTRZtBu$_2$** at λ_{PL} = 443 nm to λ_{PL} = 458 nm for **dtBuCzDCCPTRZtBu$_2$** and λ_{PL} = 475 nm for **dMeOCzDCCPTRZtBu$_2$**. The PL quantum yield (Φ_{PL}) of degassed toluene solutions of **DCCPTRZ** and **dtBuCzDCCPTRZtBu$_2$** are 91% and 89%, respectively, and showed no significant change upon exposure to oxygen, which suggests the intersystem crossing between S_1 and T_1 is negligible.[8] The transient PL of **DCCPTRZtBu$_2$**, **dtBuCzDCCPTRZtBu$_2$** and **dMeOCzDCCPTRZtBu$_2$** were found to decay monoexponentially, with lifetimes of 16 ns, 21 ns, and 29 ns, respectively; therefore, in toluene these three compounds are fluorescent. For all compounds the ΔE_{ST} in toluene was measured to be > 200 meV (**Figure S26**) and therefore unlikely to support efficient reverse intersystem crossing (RISC) at room temperature. However, upon rapid cooling using liquid nitrogen, the emitters at 77 K would be frozen in their respective non-equilibrised geometries, resulting in an overestimation of ΔE_{ST}.

The compounds were then studied as doped poly(*N*-vinyl carbazole) (PVK) films at a concentration of 10 wt%, the value of which was chosen to optimise the Φ_{PL} (**Table 1**). The steady-state PL spectra and transient PL decays of the compounds are shown in **Figure 4**. The steady-state PL spectra show the same trends as those in solution but are red-shifted with λ_{PL} = 455 nm for **DCCPTRZtBu$_2$**, λ_{PL} = 455 nm for **dtBuCzDCCPTRZtBu$_2$**, and λ_{PL} = 490 nm for **dMeOCzDCCPTRZtBu$_2$**. The Φ_{PL} for the films is around 40%, which is significantly lower than in solution. This may be due host-emitter or emitter-emitter deactivation in the films. The transient PL decays of all films show a multiexponential prompt emission with an average lifetime, τ_p, of 10 ns, 7.4 ns, and 6.8 ns for **DCCPTRZtBu$_2$**, **dtBuCzDCCPTRZtBu$_2$**, and **dMeOCzDCCPTRZtBu$_2$**, respectively. The transient PL of **dtBuCzDCCPTRZtBu$_2$**, and **dMeOCzDCCPTRZtBu$_2$** show a multiexponential delayed lifetime component with an average lifetime, τ_d, of 9.7 µs and 7.7 µs at 300 K. The delayed emission lifetime is comparable to the delayed component of **CzpPhTrz** in PVK of 9.0 µs (**Figure S25**).

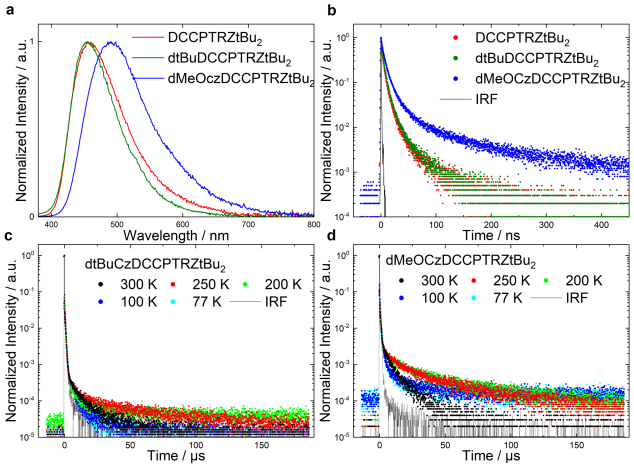

Figure 4. Photoluminescence of emitters in PVK film (10 wt%). (a) Steady-state PL spectra (λ_{exc} = 345 nm), (b) prompt PL decay of all emitters, (c) delayed PL decay component at different temperatures of **dtBuCzDCCPTRZtBu$_2$** and (d) **dMeOCzDCCPTRZtBu$_2$**. For transient PL (λ_{exc} = 378 nm).

The delayed component is longer-lived at lower temperatures and does not show a complete quenching at low temperature as expected for a TADF emitter. The ΔE_{ST} values are 110 meV and 70 meV for **dtBuCzDCCPTRZtBu$_2$**, and **dMeOCzDCCPTRZtBu$_2$**, respectively (**Figure S27**), and thus sufficiently small for TADF to be operational at room temperature. The short delayed lifetime and moderate Φ_{PL} at room temperature can be explained by a strong non-radiative decay contribution from the triplet state. At lower temperatures this pathway is quenched due to fewer vibrations resulting in a longer delayed lifetime. In the case of **dMeOCzDCCPTRZtBu$_2$**, RISC does not appear to be fully suppressed at 77 K. Assuming the previous discussed measured ΔE_{ST} = 70 meV is identical to the energy barrier for RISC in **dMeOCzDCCPTRZtBu$_2$**, we expect k_{RISC} to be reduced by four orders of magnitude at 77 K from k_{RISC} at 300 K but not entirely quenched, resulting in a long delayed emission lifetime.

Given the high molecular weights of the emitters, solution-processed devices were fabricated with the following layers: indium tin oxide (ITO) / poly(3,4-ethylenedioxythiophene) polystyrene sulfonate (PEDOT:PSS) (40 nm)/emitter:PVK (10 wt%, 35–40 nm) / 1,3,5-tris(3-pyridyl-3-phenyl)benzene (TmPyPB) (50 nm)/LiF (0.5 nm)/Al (100 nm). The electroluminescence properties are shown in **Figure S28** and the device metrics are listed in **Table S29**. Analogous to the trend observed in the PL study, the emission colour of the devices progressively red-shifts from sky-blue emission for **DCCPTRZtBu$_2$** with a λ_{EL} of 475 nm, to λ_{EL} = 478 nm for **dtBuCzDCCPTRZtBu$_2$** to λ_{EL} = 515 nm for **dMeOCzDCCPTRZtBu$_2$**. The EL spectra are greener (i.e. relatively red-shifted) than the corresponding PL spectra in the PVK host at the same doping concentration. This might be due to microcavity effects in the device.

The highest EQE_{max} was found for the device with **dMeOCzDCCPTRZtBu$_2$** at 8.2%, and this OLED achieved an efficiency of 7.9% at 100 cd/m^2. Devices with **DCCPTRZtBu$_2$** and **dtBuCzDCCPTRZtBu$_2$** exhibited much lower EQE_{max} of 3.2% and 4.0%, respectively. Based on the previous discussed PLQY of the PVK films doped with **dMeOCzDCCPTRZtBu$_2$** (Φ_{PL} = 41%) the theoretical EQE_{max} is 8.2% when considering an outcoupling efficiency of $\chi_{out} \approx 20\%$, and that all triplet excitons are efficiently converted into singlets. Therefore, we conclude that the OLED operates via an efficient TADF mechanism. The lower efficiency in devices with either **DCCPTRZtBu$_2$** or **dtBuCzDCCPTRZtBu$_2$** cannot be explained by singlet emission alone as this would lead to an expected EQE_{max} of 2.1% and 1.9%, respectively. Therefore, triplet up conversion must occur in these devices too; however, with a lower exciton utilization efficiency than in **dMeOCzDCCPTRZtBu$_2$**, which is likely due to their larger ΔE_{ST}. **DCCPTRZtBu$_2$** did not show any indication of TADF in doped films within our PL studies. As the EQE_{max} is observed at higher current densities as in the devices with **dMeOCzDCCPTRZtBu$_2$**, the upconversion might be explained by triplet-triplet annihilation, which is facilitated by a large triplet population.

In this work, we describe the design and modular synthesis of centrosymmetric **DCCP**-based through-space donors via a multi-fold stepwise Pd-catalyzed Buchwald-Hartwig amination and ring cyclization approach. The derived emitters, **DCCPTRZtBu$_2$**, **dtBuCzDCCPTRZtBu$_2$**, and **dMeOCzDCCPTRZtBu$_2$** showed Φ_{PL} of up to 91% in toluene and 41% in doped PVK films. Consequently, solution-processed OLEDs using **dMeOCzDCCPTRZtBu$_2$** were fabricated and achieved an EQE_{max} of 8.2% *via* an efficient TADF mechanism.

ASSOCIATED CONTENT

Supporting Information

The Supporting Information is available free of charge on the ACS Publications website.
Preparation, X-ray crystallography data (**1**, CCDC 2049645; **DCCP** (**2**), CCDC 2049646; **DCCP-2Br** (**3**), CCDC 2049647; and **DCCPTRZtBu$_2$**, CCDC 2049648), photophysical properties, calculation details, NMR spectra.

AUTHOR INFORMATION

Corresponding Authors

Stefan Bräse – Institute of Organic Chemistry, Karlsruhe Institute of Technology (KIT), Fritz-Haber-Weg 6, 76131 Karlsruhe, Germany. E-mail: braese@kit.edu
Eli Zysman-Colman – Organic Semiconductor Centre, EaStCHEM School of Chemistry, University of St Andrews, St Andrews, Fife, KY16 9ST, UK. E-mail: eli.zysman-colman @st-andrews.ac.uk
Ifor D. W. Samuel – Organic Semiconductor Centre, SUPA, School of Physics and Astronomy, University of St Andrews, North Haugh, St Andrews, KY16 9SS, UK. E-mail: idws@st-andrews.ac.uk

Authors

Zhen Zhang – Institute of Organic Chemistry, Karlsruhe Institute of Technology (KIT), Fritz-Haber-Weg 6, 76131 Karlsruhe, Germany.
Stefan Diesing – Organic Semiconductor Centre, EaStCHEM School of Chemistry, University of St Andrews, St Andrews, Fife, KY16 9ST, UK.
Ettore Crovini – Organic Semiconductor Centre, EaStCHEM School of Chemistry, University of St Andrews, St Andrews, Fife, KY16 9ST, UK.
Abhishek Kumar Gupta – Organic Semiconductor Centre, EaStCHEM School of Chemistry, University of St Andrews, St Andrews, Fife, KY16 9ST, UK.
Eduard Spuling – Institute of Organic Chemistry, Karlsruhe Institute of Technology (KIT), Fritz-Haber-Weg 6, 76131 Karlsruhe, Germany.
Xuemin Gan – Institute of Organic Chemistry, Karlsruhe Institute of Technology (KIT), Fritz-Haber-Weg 6, 76131 Karlsruhe, Germany.
Olaf Fuhr – Institute of Nanotechnology (INT) and Karlsruhe Nano-Micro Facility (KNMF), Karlsruhe Institute of Technology (KIT), Hermann-von-Helmholtz-Platz 1, 76344 Eggenstein-Leopoldshafen, Germany
Martin Nieger – Department of Chemistry, University of Helsinki, P.O. Box 55 A.I. Virtasen aukio 1, 00014 University of Helsinki, Finland
Zahid Hassan – Institute of Organic Chemistry, Karlsruhe Institute of Technology (KIT), Fritz-Haber-Weg 6, 76131 Karlsruhe, Germany.

Zhen Zhang‡ and **Stefan Diesing**‡ contributed equally to this work.

Notes

The authors declare no competing financial interest.

ACKNOWLEDGMENT

The German Research Foundation (formally Deutsche Forschungsgemeinschaft DFG) in the framework of SFB1176 Cooperative Research Centre "Molecular Structuring of Soft Matter" (CRC1176, A4, B3, C2, C6) and the cluster "3D Matter Made to Order" all funded under Germany's Excellence Strategy 2082/1–390761711 are acknowledged for financial contributions. A. K. G. is thankful to the Royal Society for a Newton International Fellowship NF171163. E. Z.-C. and I. D. W. S. acknowledge support from EPSRC (EP/L017008, EP/P010482/1, EP/R035164/1). E. C. and E. Z.-C. acknowledge the EU Horizon 2020 grant agreement no. 812872 (TADFlife).

REFERENCES

(1). (a) Cram, D. J.; Cram, J. M. Cyclophane Chemistry: Bent and Battered Benzene Rings. *Acc. Chem. Res.* **1971**, *4*, 204–213. (b) Zyss, J.; Ledoux, I.; Volkov, S.; Chernyak, V.; Mukamel, S.; Bartholomew, G. P.; Bazan, G. C. Through-Space Charge Transfer and Nonlinear Optical Properties of Substituted Paracyclophane. *J. Am. Chem. Soc.* **2000**, *122*, 11956–11962. (c) Hong, J. W.; Woo, H. Y.; Liu, B.; Bazan, G. C. Solvatochromism of Distyrylbenzene Pairs Bound Together by [2.2]Paracyclophane: Evidence for a Polarizable "Through-Space" Delocalized State. *J. Am. Chem. Soc.* **2005**, *127*, 7435–7443. (d) Morisaki, Y.; Chujo, Y. Through-space conjugated polymers consisting of [2.2]paracyclophane. *Polym. Chem.* **2011**, *2*, 1249–1257. (e) Morisaki, Y.; Chujo, Y. π-Electron-system-layered polymers based on [2.2]paracyclophane. *Chem. Lett.* **2012**, *41*, 840-846. (f) Morisaki, Y.; Gon, M.; Sasamori, T.; Tokitoh, N.; Chujo, Y. Planar chiral tetrasubstituted [2.2]paracyclophane: optical resolution and functionalization. *J. Am. Chem. Soc.* **2014**, *136*, 3350–3353. (g) Gon, M.; Morisaki, Y.; Chujo, Y. A silver(i)-induced higher-ordered structure based on planar chiral tetrasubstituted [2.2]paracyclophane. *Chem. Commun.* **2017**, *53*, 8304–8307. (h) Hassan, Z.; Spuling, E.; Knoll, D. M.; Lahann, J.; Bräse, S. Planar chiral [2.2]paracyclophanes: from synthetic curiosity to applications in asymmetric synthesis and materials. *Chem. Soc. Rev.* **2018**, *47*, 6947–6963. (i) Zhang, M. Y.; Li, Z. Y.; Lu, B.; Wang, Y.; Ma, Y. D.; Zhao, C. H. Solid-state emissive triarylborane-based [2.2]paracyclophanes displaying circularly polarized luminescence and thermally activated delayed fluorescence. *Org. Lett.* **2018**, *20*, 6868–6871. (j) Zhang, M. Y.; Liang, X.; Ni, D. N.; Liu, D. H.; Peng, Q.; Zhao, C. H. 2-(Dimesitylboryl)phenyl-substituted [2.2]paracyclophanes featuring intense and sign-invertible circularly polarized luminescence. *Org. Lett.* **2021**, *23*, 2–7.

(2). (a) Bartholomew, G. P.; Bazan, G. C. Bichromophoric Paracyclophanes: Models for Interchromophore Delocalization. *Acc. Chem. Res.* **2001**, *34*, 30–39. (b) Marrocchi, A.; Tomasi , I.; Vaccaro, L. Organic small molecules for photonics and electronics from the [2.2]paracyclophane scaffold. *Isr. J. Chem.* **2012**, *52*, 41–52. (c) Spuling, E.; Sharma, N.; Samuel, I. D. W.; Zysman-Colman, E.; Brase, S. (Deep) blue through-space conjugated TADF emitters based on [2.2]paracyclophanes. *Chem. Commun.* **2018**, *54*, 9278–9281. (d) Wang, C. S.; Wei, Y. C.; Chang, K. H.; Chou, P. T.; Wu, Y. T. Indeno[1,2-b]fluorene-based [2,2]cyclophanes with 4n/4n and 4n/[4n+2] pi electrons: syntheses, structural analyses, and excitonic coupling properties. *Angew. Chem. Int. Ed.* **2019**, *58*, 10158–10162. (e) Liang, X.; Liu, T. T.; Yan, Z. P.; Zhou, Y.; Su, J.; Luo, X. F.; Wu, Z. G.; Wang, Y.; Zheng, Y. X.; Zuo, J. L. Organic Room-Temperature Phosphorescence with Strong Circularly Polarized Luminescence Based on Paracyclophanes. *Angew. Chem. Int. Ed.* **2019**, *58*, 17220–17225. (f) Hassan, Z.; Spuling, E.; Knoll, D. M.; Brase, S. Regioselective Functionalization of [2.2]Paracyclophanes: Recent Synthetic Progress and Perspectives. *Angew. Chem. Int. Ed.* **2020**, *59*, 2156–2170.

(3). Sharma, N.; Spuling, E.; Mattern, C. M.; Li, W.; Fuhr, O.; Tsuchiya, Y.; Adachi, C.; Brase, S.; Samuel, I. D. W.; Zysman-Colman, E. Turn on of sky-blue thermally activated delayed fluorescence and circularly polarized luminescence (CPL) via increased torsion by a bulky carbazolophane donor. *Chem. Sci.* **2019**, *10*, 6689–6696.

(4). Liao, C.; Zhang, Y.; Ye, S. H.; Zheng, W. H. Planar Chiral [2.2]Paracyclophane-Based Thermally Activated Delayed Fluorescent Materials for Circularly Polarized Electroluminescence. *ACS Appl. Mater. Interfaces* **2021**, *13*, 25186–25192.

(5). Gupta, A. K.; Zhang, Z.; Spuling, E.; Kaczmarek, M.; Wang, Y.; Hassan, Z.; Samuel, I. D. W.; Bräse, S.; Zysman-Colman. E. Electron-withdrawing Group Modified Carbazolophane Donors for Deep Blue Thermally Activated Delayed Fluorescence OLEDs. *J. Mater. Chem. C* **2021**, *submitted*.

(6). (a) Lennartz, P.; Raabe, G.; Bolm, C. Synthesis of Planar Chiral Carbazole Derivatives Bearing a [2.2]Paracyclophane Skeleton. *Isr. J. Chem.* **2012**, *52*, 171–179. (b) Buchwald, S. L.; Huang, W. [2-2]paracyclophane-derived donor/acceptor type molecular for OLED applications. WO2016196885 A1.

(7). (a). Santos, P. L.; Ward, J. S.; Data, P.; Batsanov, A. S.; Bryce, M. R.; Dias, F. B.; Monkman, A. P. Engineering the singlet–triplet energy splitting in a TADF molecule. *J. Mater. Chem. C* **2016**, *4*, 3815–3824. (b) Hosokai, T.; Matsuzaki, H.; Nakanotani, H.; Tokumaru, K.; Tsutsui, T.; Furube, A.; Nasu, K.; Nomura, H.; Yahiro, M.; Adachi, C. Evidence and mechanism of efficient thermally activated delayed fluorescence promoted by delocalized excited states. *Sci. Adv.* ***2017***, 3, e1603282. (c) Noda, H.; Nakanotani, H.; Adachi, C. Excited state engineering for efficient reverse intersystem crossing. *Sci. Adv.* **2018**, 4, eaao6910. (d) Samanta, P. K.; Kim, D.; Coropceanu, V.; Bredas, J. L. Up-Conversion Intersystem Crossing Rates in Organic Emitters for Thermally Activated Delayed Fluorescence: Impact of the Nature of Singlet vs Triplet Excited States. *J. Am. Chem. Soc.* **2017**, *139*, 4042–4051.

(8). (a) Melhuish, W. H. Quantum Efficiencies of Fluorescence of Organic Substances : Effect of Solvent and Concentration of the Fluorescent solute. *J. Phys. Chem.* **1961**, *65*, 229–235. (b) Demas, J. N.; Crosby, G. A. The Measurement of Photoluminescence Quantum Yields. *J. Phys. Chem.* **1971**, *75*, 991–1024.